

Freshly etched porous silicon as counter electrode of dye sensitized solar cells

L.-L. Chen & S.-Z. Wang

To cite this article: L.-L. Chen & S.-Z. Wang (2015) Freshly etched porous silicon as counter electrode of dye sensitized solar cells, Materials Research Innovations, 19:sup7, s21-s24, DOI: [10.1179/1432891715Z.0000000002046](https://doi.org/10.1179/1432891715Z.0000000002046)

To link to this article: <http://dx.doi.org/10.1179/1432891715Z.0000000002046>



Published online: 15 Sep 2015.



Submit your article to this journal [↗](#)



Article views: 34



View related articles [↗](#)



View Crossmark data [↗](#)

Freshly etched porous silicon as counter electrode of dye sensitized solar cells

L.-L. Chen* and S.-Z. Wang

Freshly etched porous silicon films are explored as the counter electrodes of TiO₂-based dye-sensitised solar cells (DSSCs). The scanning electron microscope characterisations show that the 12- μ m-thick porous silicon film has pores in the diameter of about 50 nm. Under AM1.5 illumination, the DSSCs with porous silicon electrodes exhibited an efficiency of 1.43% in contrast to the 5.5% of the control DSSC constructed with a platinum (Pt) counter electrode. The impedance study reveals that the porous silicon electrode has larger series and charge transfer resistances than those of the Pt counter electrode, while the cyclic voltammograms indicate that porous silicon exhibits moderate electrocatalytic activity. Our results have demonstrated that porous silicon films are helpful to be the counter electrodes of moderately efficient DSSCs.

Keywords: Porous silicon, Dye-sensitised solar cells, Counter electrode, Photovoltaic performance

Introduction

Dye-sensitized solar cells (DSSCs) have been considered as potential candidates for next-generation solar cells owing to its low production cost and reasonable high efficiency.^{1,2} A typical DSSC comprises a dye-sensitised semiconductor photoanode, a redox couple containing electrolyte and a platinised counter electrode.^{3,4} The counter electrode is an important element in the DSSCs because it collects electrons from the external circuit and catalyses the conversion of I₃⁻ to I⁻ in the electrolyte. At present, platinum (Pt) films are widely utilised as the counter electrode in most DSSCs owing to their good conductivity, excellent electrocatalytic activity and chemical stability. However, Pt is an expensive noble metal; its high price and low abundance on the earth hamper the large-scale production and long-term application of DSSCs. Therefore, it is important to develop low-cost and Pt-free counter electrode materials. So far, a variety of Pt-free counter electrodes were reported, including carbon black,⁵ carbon nanotube,⁶ carbon black/polymer composites,⁷ carbon nanotube/polymer composites,⁸ and graphene/polymer composites.⁹ Through these carbon-based counter electrode materials and electrons from external circuit are transferred back to the redox electrolyte for the reduction reactions.

Being an important semiconducting material with tunable surface morphology, porous Si (PS) is well known for its easy fabrication, large specific surface area, good electrical conductivity and abundance on the earth.^{10,11} In the early work, PS was reported to exhibit moderate electrocatalytic activity owing to its reduction

of metallic ions into metallic nanoparticles on its vast surface.¹²⁻¹⁴ Recently, Erwin *et al.* demonstrated the use of carbon passivated PS counter electrodes in DSSCs with an efficiency of 5.38%.² These results suggested carbon-modified PS as a promising alternative to rare metals for the counter electrodes in DSSCs.² However, the exact contribution of PS to the efficiency of the solar cells is still unknown because the carbon-based materials are in themselves efficient counter electrodes in DSSCs.⁵⁻⁹ For example, Xu *et al.* reported a high efficiency of 4.03% for the DSSC with a mesoscopic carbon counter electrode.⁵ In order to assess the direct contribution of PS in the DSSCs, we investigated the freshly etched PS film as the counter electrode of DSSCs. Our results demonstrated that DSSCs constructed with a 12- μ m-thick PS counter electrode achieved an efficiency of 1.43%, which was about 26% of the efficiency of a control DSSC with a Pt counter electrode (5.5%).

Experimental details

Preparation of TiO₂ anode

Fluorine doped tin oxide (FTO) glass plates (Wuhan Geao Co., Ltd) were used as the electrode substrates for our DSSCs. The sheet resistance and the thickness of the FTO glass substrates were about 14 Ω cm⁻² and 2.2 mm, respectively. Four steps were taken to prepare a TiO₂ anode on the FTO glass. Step 1: a compact TiO₂ layer of around 40 nm thickness was deposited on the FTO substrate by immersing it into an aqueous solution of TiCl₄ (40 mM) at 70°C for 30 min, then the FTO substrate was sintered in a furnace at 450°C for 30 min. Step 2: a 14- μ m-thick porous TiO₂ layer (P25, Degussa) was coated onto the FTO substrate via the doctor blade technique, which was followed by the second sintering at 450°C in air for 30 min. Step 3: the TiO₂ layer was treated by another 40 mM TiCl₄ immersion, which was followed by the third sintering at 450°C for 30 min. Step 4: the TiO₂ anode was

School of Electronic and Electrical Engineering, Nanyang Institute of Technology, Nanyang 473006, Henan, China

*Corresponding author, email chlanli@126.com

immersed into the 0.4 mM ethanol solution of the N-719 dye (Shanghai MaterWin New Materials Ltd, Shanghai, China) for 10 hours.

Preparation of PS counter electrode

The PS film of about 12 μm thickness was prepared by electrochemical anodisation of boron doped p-type (111)-oriented Si wafer in hydrofluoric electrolyte.^{10,11} The resistivity of the Si wafer was in the range of 8–13 $\Omega\text{ cm}$. The electrolyte was an equal volume mixture of hydrofluoric acid (40 wt-%) and ethanol (98 wt-%). Platinum wire was utilised as the counter electrode while the Si wafer was employed as the working electrode. The anodising current density was 10 mA cm^{-2} and its duration was 60 minutes. The freshly etched PS film was rinsed in ethanol repeatedly and then dried in an oven before it was assembled into a DSSC as the counter electrode.

DSSC fabrication

The sensitised TiO_2 anode and the PS counter electrode were thermally sealed into a sandwiched structure with a 25- μm -thick thermobonding Surlyn gasket (Dupont, Torrance, California, USA). The free space in the sandwiched structure was filled with the acetonitrile solution of KI (500 mM) and I_2 (50 mM). The iodide/triiodide based electrolyte was injected into the sandwiched cell through a laser-drilled hole. The hole was subsequently sealed by heating a piece of Surlyn-attached glass onto the hole with a hot iron. Finally, two fine copper wires were attached to the photoanode and the counter electrode for J - V measurements. In addition to the PS based DSSC, a control DSSC was prepared by making use of Pt counter electrode. A cleaned FTO substrate was dipped into the 4 mM ethanol solution of H_2PtCl_6 (Sinopharm Chemical Reagents Co., Ltd, Shanghai, China) for 1 min, pulled out and then dried in an oven at 80°C for 10 min. Such dipping–pulling–drying process was cycled for five times. Finally the Pt film was calcined at 450°C for 2 h to form a Pt counter electrode. The thickness of the Pt film was about 100 nm.^{3,4} The control DSSC was prepared by assembling the TiO_2 based photoanode and the Pt counter electrode into a sandwiched structure as described above. The active area of each photoanode was 1 cm^2 .

Characterization

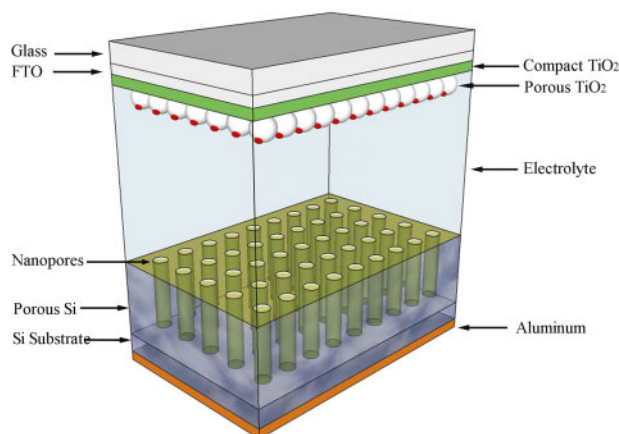
A field-emission scanning electron microscope (FE-SEM, SUPPRA 55, Zeiss, Germany) was utilised to characterise the surface morphologies of the counter electrodes. An AM1.5 solar simulator with a 500 W xenon lamp was employed to illuminate the DSSCs, the incident light power was calibrated to 100 mW cm^{-2} . An area of 0.25 cm^2 on the photoanode was illuminated, in the meanwhile the remainder was covered with a shadow mask. DSSCs were tested over a potential range of -1 to $+1$ V at a scan rate of 50 mV s^{-1} under AM1.5 illumination. Electrochemical impedance measurements were performed over a frequency range of 10^{-1} – 10^5 Hz with a 10 mV peak-to-peak sinusoidal perturbation under dark condition at 25°C. (EZstat-Pro EIS, NuVant Systems, Crown Point, Indiana, USA). Cyclic voltammetry (CV) measurements were carried out in a three-electrode setup with a Pt counter electrode and a saturated calomel reference electrode (SCE). The acetonitrile solution

containing 50 mM of KI and 5 mM of I_2 was used as an electrolyte in both the impedance and the CV measurements.

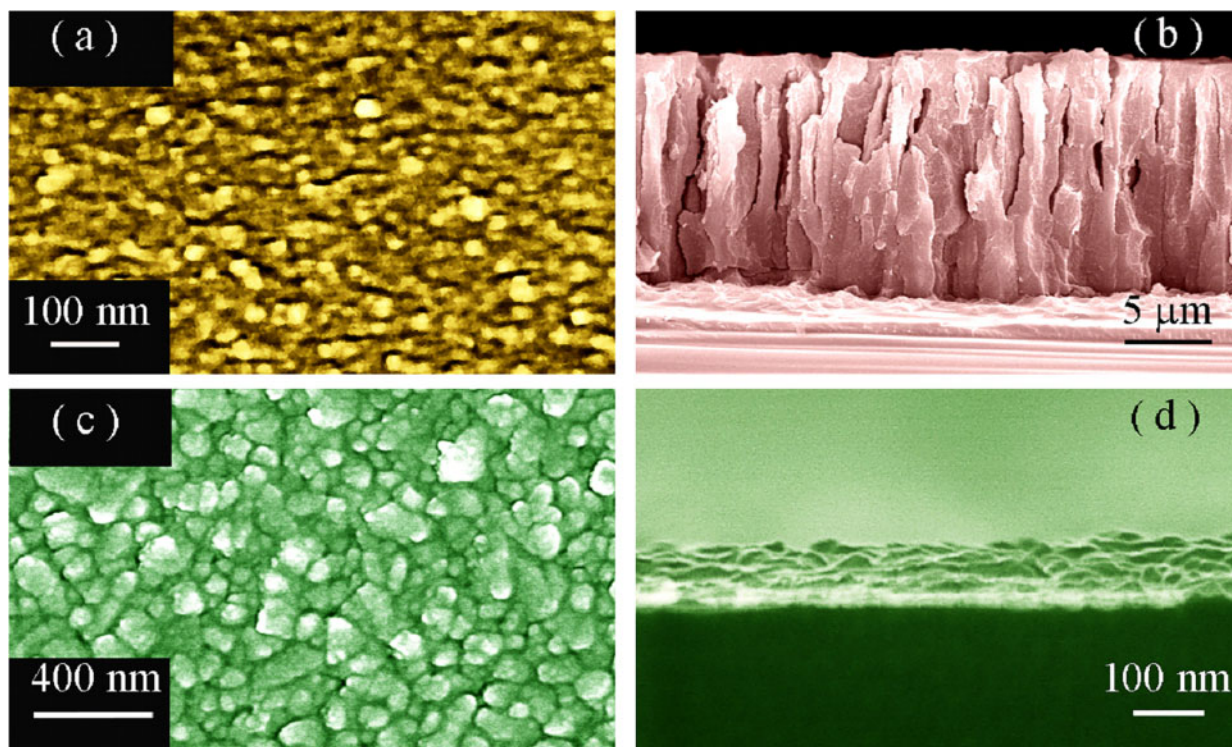
Results and discussion

The schematic illustration of the geometrical structure of the DSSC is depicted in Fig. 1. The photoanode is composed of one compact TiO_2 layer and one porous TiO_2 layer on the FTO glass substrate. With the characterisation of SEM, the thicknesses of the compact TiO_2 layer and the porous TiO_2 layer were measured to be about 40 nm and 14 μm , respectively. The red dots on the porous TiO_2 layer in the photoanode represent the molecules of the N719 dye. The counter electrode comprises PS film, the unetched Si substrate and an aluminium film. The PS is characteristic of many nanoscale pores.^{10,11} The potential interest of PS as the counter electrode for DSSCs stems from the nature of the porous structures in the film. On one hand, the channels in PS renders the iodide and triiodide ions to be transferred into Si pores at a molecular level and have intimate contacts with the reduction sites on the Si nanoparticles. On the other hand, the quasi one-dimensional Si columns provide a direct electron pathway from external circuit to the electrolyte. In particular, the large specific surface area of the PS makes the catalytic activity higher. Therefore, the PS films are expected to exhibit reasonable electrocatalytic activity.

The top and cross-sectional SEM micrographs of the PS counter electrode (a, b) and the Pt counter electrode (c, d) are shown in Fig. 2. It is clear in Fig. 2a that the top surface of the PS film is featured with a lot of nanopores, whose diameter is around 50 nm. Figure 2b reveals the columnar pillars and microchannels in the PS film. These microchannels are perpendicular to the Si substrate. Both the microchannels and the nanopores make the porous matrix suitable for the infiltration of the electrolyte by the capillary action. Once the iodide/triiodide ions are sucked onto the surface of Si nanocrystals, they are ready for the electrocatalytic reactions. By contrast, Fig. 2c and d shows that the average size of the Pt nanocrystals is around 50 nm and the thickness of the Pt counter electrode is about 100 nm. It is obvious that no nanochannels are present in the Pt counter electrode. A comparison of the graphs in Fig. 2 indicates



1 Schematic illustration of the structure of a DSSC with PS counter electrode



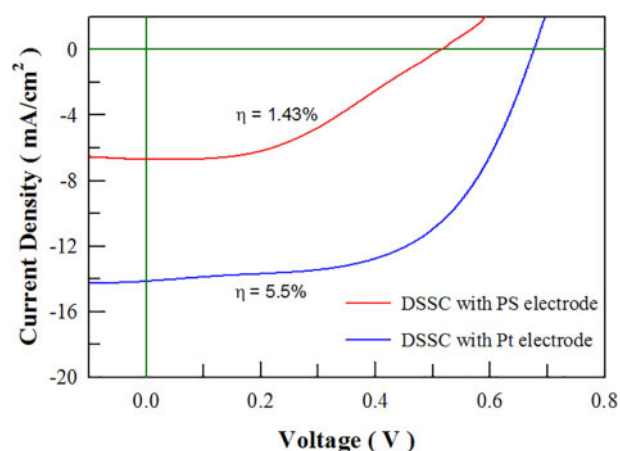
2 Top and sectional SEM micrographs: *a, b* the PS counter electrode; *c, d* the Pt counter electrode

that PS electrode has larger specific surface area than the Pt counter electrode owing to the presence of nanopores and quasi one-dimensional columnar pillars in PS.

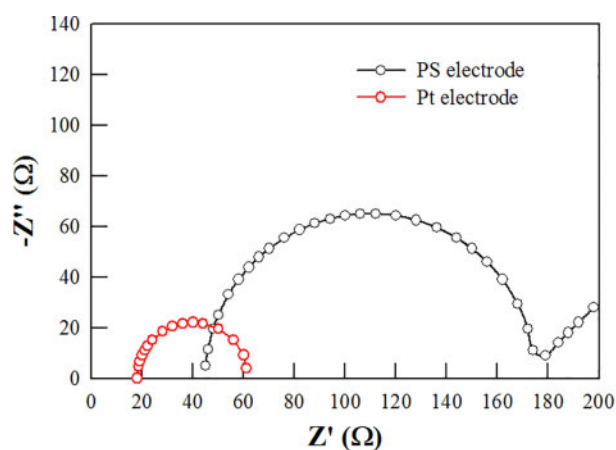
Figure 3 presents the J - V curves of the DSSC constructed with a PS counter electrode and the DSSC constructed with a Pt counter electrode. The short-circuit current density, open-circuit voltage, fill factor and calculated efficiency of the PS-based DSSC are 6.69 mA cm^{-2} , 0.520 V , 0.411 and 1.43% , respectively. By contrast, those for the control DSSC are 14.16 mA cm^{-2} , 0.68 V , 0.571 and 5.5% , respectively. It is clear that the efficiency of the PS-based DSSC is about 26% of that of the Pt-based DSSC. These data in Fig. 3 have demonstrated that the DSSC with a PS counter electrode exhibits lower efficiency when compared to the DSSC constructed with a Pt electrode. Authors also note that the open circuit voltage of the DSSCs fabricated

with PS electrode is lower than that of the DSSC constructed with a Pt electrode. The large resistances and lower catalytic activity of Si nanocrystals are proposed to be responsible for the lower photovoltaic performance of the PS-based DSSC owing to the surface corrosion of Si nanoparticles in the electrolyte. Although the efficiency of the PS-based DSSC is not competitive to the Pt-based DSSC, the significance, in Fig. 3, rests on that PS can act as the counter electrode of the DSSC after consideration of the Si abundance in earth. Furthermore, the scientific merits of Si-based DSSCs lie in the fact that it helps the development of Pt-free solar cells.

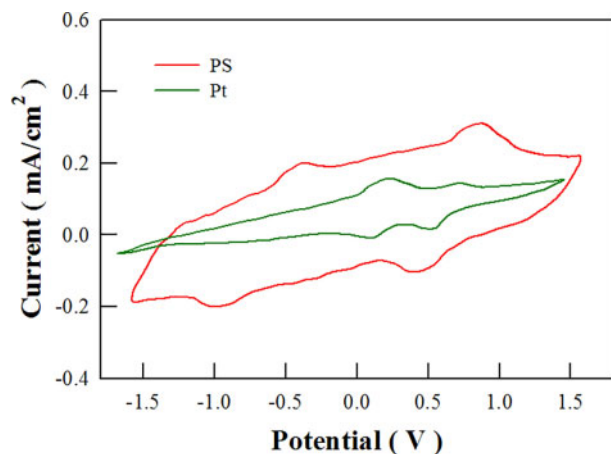
In order to investigate the charge transfer properties in the system, the PS counter electrodes were characterised with the electrochemical impedance spectroscopy. Figure 4 depicts the electrochemical impedance spectra of the PS electrode and the Pt



3 J-V curves of the DSSCs with PS counter electrode and the Pt counter electrode under the illumination of one sun



4 Nyquist plots of the PS and Pt electrodes under zero voltage bias over a frequency range of 0.1 to 100,000 Hz



5 Cyclic voltammograms of PS and Pt electrodes

electrode over a frequency range of 10^{-1} – 10^5 Hz. The semicircles in Fig. 4 represent the charge-transfer resistance and double-layer capacitance at the cathode. Series and charge-transfer resistances can be calculated on the basis of the Randles model. From the data in Fig. 4, the series and charge-transfer resistances of the PS are derived to be 45 and 130Ω while those of the Pt electrode are 18 and 44Ω , respectively. Relative to the planar Pt, the DSSC constructed with the PS counter electrode exhibits higher series and charge-transfer resistances. The higher series resistance of the Si-based DSSC stems from the corrosion occurring on exposed Si surface,² its higher charge-transfer resistance indicates slower ionic diffusion and hence slower kinetics of triiodide reduction.

To further understand the electrochemical properties of the PS electrodes, CV measurements were carried out in a three-electrode setup. Figure 5 illustrates the cyclic voltammograms of PS and Pt electrodes. These scans were recorded in a potential window of -1.7 to 1.7 V (Ag/AgCl) at scan rate of 50 mV s^{-1} . The CV curve of the Pt counter electrode is similar to that found in the literature.² Two sets of peaks were observed in the CV curve of the Pt counter electrode, which corresponds to the reduction of iodine to triiodide given by redox reactions 1 and reduction of triiodide to iodide ions given by reaction 2



Similarly, two sets of peaks were observed in the CV curve of the PS counter electrode. It is obvious that PS showed redox peaks at around 1.0 V (Ag/AgCl) in both directions, which are consistent with the redox peaks of PS in literature.¹⁵ The separation of the reduction and oxidation peaks is indicative of the electrochemical catalytic activity of the counter electrodes. On one hand, the cyclic voltammograms in Fig. 5 indicate that the separation of the reduction and oxidation peaks of the PS electrode is larger than that of the Pt electrode, suggesting the lower electrocatalytic ability of PS for the I^-/I_3^- redox couple with relative to the Pt electrode. On the other hand, the cathodic reduction peak currents of the PS electrode are a little bit larger than those of the planar Pt electrode.

Such an increase in the cathodic reduction peak currents can enhance the electrocatalytic activity of the PS electrode. The data in Fig. 5 have demonstrated that the overall catalytic activity of the PS electrode is moderate when compared to the excellent catalytic activity of the Pt electrode. Since, the surface of fresh porous silicon can be oxidised easily, such oxidation can deteriorate the photovoltaic performance of the DSSCs. Authors monitored the evolutions of J - V curves of the DSSCs with the illumination time. The efficiency of the DSSCs decreased to 1.0% under the illumination for 28 min, and the efficiency was decreased further to 0.7% was recorded under the illumination for 80 min.

Conclusion

In summary, we have demonstrated the freshly etched PS materials as a counter electrode for DSSCs with an efficiency of 1.43% and moderate catalytic activity. Electrochemical impedance studies have indicated that the larger series and charge transfer resistances of porous Si electrode are responsible for the lower efficiency of the Si-based DSSC. Although the efficiency of the Si-based DSSC is not comparable to that of the Pt-based DSSC, freshly etched PS is the starting point for surface engineered PS electrodes. Owing to the tunable surface properties of PS films, the surface modification of PS is helpful to reduce the resistances of the PS electrode, which can in turn lead to improved efficiency for Si-based DSSCs.

Acknowledgements

This work was supported by the Natural Science Foundation of Henan Province (No. 122300410205).

References

1. B. O'Regan and M. Grätzel: *Nature*, 1991, **353**, 737–740.
2. W. R. Erwin, L. Oakes, S. Chatterjee, H. F. Zarick, C. L. Pint and R. Bardhan: *ACS Appl. Mater. Inter.*, 2014, **6**, 9904–9910.
3. L. Yang, Q. L. Ma, Y. G. Cai and Y. M. Huang: *Appl. Surf. Sci.*, 2014, **292**, 297–300.
4. L. Yang, B. G. Zhai, Q. L. Ma and Y. M. Huang: *J. Alloy. Compd.*, 2014, **605**, 109–112.
5. M. Xu, G. Liu, X. Li, H. Wang, Y. Rong, Z. Ku, M. Hu, Y. Yang, L. Liu, T. Liu, J. Chen and H. Han: *Org. Electron.*, 2013, **14**, 628–634.
6. J. Han, H. Kim, D. Y. Kim, S. M. Jo and S. -Y. ACS: *Nano*, 2010, **4**, 3503–3509.
7. W. Huang, X. L. Zhang, F. Huang, Z. Zhang, J. He and Y. -B. Cheng: *J. Nanopart. Res.*, 2012, **14**, 838.
8. Z. Yang, T. Chen, R. He, H. Li, H. Lin, L. Li, G. Zou, Q. Jia and H. Peng: *Polym. Chem.*, 2013, **4**, 1680–1684.
9. G. Yue, J. Wu, Y. Xiao, J. Lin, M. Huang, Z. Lan and L. Fan: *Energy*, 2013, **54**, 315–321.
10. Q. L. Ma, R. Xiong and Y. M. Huang: *J. Lumin.*, 2011, **131**, 2053–2057.
11. Y. M. Huang, F. F. Zhou, B. G. Zhai and L. -L. Chen: *Solid State Ion.*, 2008, **179**, 1194–1197.
12. I. Coulthard, D. -T. Jiang, J. W. Lorimer, T. K. Sham and X. -H. Feng: *Langmuir*, 1993, **9**, 3441–3445.
13. I. Coulthard and T. K. Sham: *Solid State Commun.*, 1998, **105**, 751–754.
14. I. Coulthard, R. Sammynaiken, S. J. Naftel, P. Zhang and T. K. Sham: *Phys. Status Solidi A*, 2000, **182**, 157–162.
15. R. K. Sharma, A. C. Rastogi and S. B. Desu: *Physica B*, 2007, **388**, 344–349.